

Practical Implementation of Attitude-Control Algorithms for an Underactuated Satellite

Horri, N. and Palmer, P.

Author post-print (accepted) deposited in CURVE November 2015

Original citation & hyperlink:

Horri, N. and Palmer, P. (2012) Practical Implementation of Attitude-Control Algorithms for an Underactuated Satellite. *Journal of Guidance, Control, and Dynamics*, volume 35 (1): 40-45.

<http://dx.doi.org/10.2514/1.54075>

Publisher statement: Copyright © 2011 by the American Institute of Aeronautics and Astronautics Inc.

Copyright © and Moral Rights are retained by the author(s) and/ or other copyright owners. A copy can be downloaded for personal non-commercial research or study, without prior permission or charge. This item cannot be reproduced or quoted extensively from without first obtaining permission in writing from the copyright holder(s). The content must not be changed in any way or sold commercially in any format or medium without the formal permission of the copyright holders.

This document is the author's post-print version, incorporating any revisions agreed during the peer-review process. Some differences between the published version and this version may remain and you are advised to consult the published version if you wish to cite from it.

CURVE is the Institutional Repository for Coventry University

<http://curve.coventry.ac.uk/open>

Practical implementation of attitude control algorithms for an underactuated satellite

Nadjim M. Horri ^{*} Phil Palmer [†]

The challenging problem of controlling the attitude of satellites subject to actuator failures has been the subject of increased attention in recent years. The problem of controlling the attitude of a satellite on all three axes with two reaction wheels is addressed in this paper. This system is controllable in a zero momentum mode. Three axis attitude stability is proven by imposing a singular quaternion feedback law to the angular velocity trajectories.

Two approaches are proposed and compared to achieve three axis control: The first one does not require angular velocity measurements and is based on the assumption of a perfect zero momentum, while the second approach consists of tracking the desired angular velocity trajectories. The full state feedback is a nonlinear singular controller. In-orbit tests of the first approach provide an unprecedented practical proof of three axis stability with two control torques. The angular velocity tracking approach is shown to be less efficient using the nonlinear singular controller. However, when inverse optimization theory is applied to enhance the nonlinear singular controller, the angular velocity tracking approach is shown to be the most efficient. The resulting switched inverse optimal controller allows for a significant enhancement of settling time, for a prescribed level of the integrated torque.

I. Introduction

Recent advances in satellite technology and in control techniques have lead to an increase in attitude control capabilities of small satellites. These improvements include higher precision pointing, higher agility and better robustness to uncertainties and disturbances. However, most of these results assume that the spacecraft is actively controlled with a number of actuators at least equal to the number of the degrees of freedom of the system.

Actuator failures onboard satellites have caused severe and even disastrous consequences on several space missions. Having redundant actuators is an expensive alternative that does not solve the problem

^{*}Research Fellow, Surrey Space Centre, University of Surrey, Guildford, GU2 7XH, U.K.

[†]Reader, Surrey Space Centre, University of Surrey, Guildford, GU2 7XH, U.K., AIAA member

completely since these may also fail. One actuator failure sometimes increases the probability of more failures in practice, as in the case of the Fuse satellite that lost two wheels. The risk of reaction wheel failures and other momentum exchange devices in particular is far from negligible. Examples include the SSTL mini-satellite UoSAT-12, the BIRD micro-satellite, Radarsat-1 and even large spacecrafts, such as GOES-9, GPS BII-07, Echostar V, Mir, Galaxy IV, Hubble.

Three axis stabilization of an underactuated satellite with two remaining control torques following an actuator failure is a challenging problem since the control system is nonholonomic. Such systems were proven by Brockett¹ to be uncontrollable using smooth (continuous and time invariant) control laws.

The paper of Crouch² was the first to investigate the dynamic and kinematic equations and controllability conditions for a rigid body using one, two or three independent control torques.

Under specific restrictions on the initial angular momenta, three axis stabilization was shown to be feasible with two control torques from thrusters³ (with zero angular velocity along unactuated axis) and reaction wheels (under zero total momentum). The less ambitious objective of dumping the angular velocities on all three axes with two control torques was considered in several references.⁴⁻⁷

Using a new parametrization of attitude kinematics,⁸ Tsiotras et al. have solved various underactuated spacecraft attitude control problems with pairs of thrusters. These included the spin stabilization of axisymmetric spacecraft, control laws with bounded inputs⁹ and optimal control laws for axisymmetric spacecrafts with restrictions on initial velocities.¹⁰ Three axis converging control laws were also proposed by Tsiotras et al. for the case of an asymmetric spacecraft.¹¹ Other authors also applied nonlinear control techniques such as quaternion based sliding mode control for underactuated satellites with thrusters,¹²⁻¹⁴ but the proposed controllers did not allow for exponential convergence of the unactuated axis attitude, unlike the singular control approach.¹⁵

In the case of momentum exchange devices, the symmetry or asymmetry of the spacecraft is not a factor. The satellite is however only controllable by two wheels under the condition of a zero total angular momentum. S.Kim and Y.Kim have proposed a control law for the spin axis stabilization of a spacecraft with two reaction wheels, using the Rodrigues-Gibbs attitude parametrization.¹⁶ Based on the same attitude parameterization, three axis stability was also shown by Yamada et al. using a continuous but time varying law.¹⁷ Terui et al. considered the bias momentum case with two wheels but practical implementation showed stability issues.¹⁸ In-Ho Seo et al.¹⁹ also considered the two wheels control problem, but with an emphasis on momentum and angular velocity control rather than attitude control.

The aim of this paper is to extend the results of the singular Tsiotras control approach, which was developed for underactuated control with thrusters in order to propose a singular quaternion feedback approach for 3-axis attitude stabilization with two wheels. The proposed controllers will be based on the genera-

tion of desirable angular velocity trajectories. Stability will be proven mathematically and demonstrated in-orbit. Another objective is to apply inverse optimal control theory to the underactuated satellite in order to enhance the performance tradeoff between integrated torque and settling time, compared to the singular converging feedback law and particularly on the unactuated axis. Indeed, some researchers have considered complementing the two wheels with magnetic torquing²⁰ to control the unactuated axis, but the limitation in this case is that magnetic torquers do not allow fast maneuvers about the unactuated axis due to their limited torque capability.

In this paper, a nonlinear quaternion feedback singular controller, based on the zero momentum condition, is first designed for stabilization of the satellite on all three axes using two wheels. A similar singular controller was proposed by Tsiotras but the attitude parameterization in that paper was subject to singularities, which are avoided here using quaternions. The controller uses feedback of the attitude only. It is both simulated and tested in-orbit.

To exploit the angular velocity feedback and relax the perfect zero momentum restriction, a full state feedback singular nonlinear controller (snlc) is constructed, based on angular velocity tracking. This approach will initially be shown to deliver relatively poor performance. The performance tradeoff between torque expenditure and settling time will however be enhanced significantly by applying inverse optimization to this angular velocity tracking controller.

In the inverse optimal control approach, a stabilizing or converging feedback law, known here as the benchmark controller, is first designed. The snlc controller is taken to be the benchmark controller. An optimization problem is then formulated to determine how the benchmark controller can be modified to solve a nonlinear programming problem, which is equivalent to minimizing a meaningful cost function. The inverse optimal controller solves a Hamilton Jacobi-Bellman (HJB) equation,²¹ representing the global formulation of the nonlinear optimal control problem. This HJB equation would otherwise be numerically intractable. The inverse optimal controller is designed to ensure stability, which is an advantage compared to other optimization techniques, especially for the underactuated satellite. Inverse optimality was applied to satellite attitude control by Krstic and Tsiotras using a continuous control law²³ and by Bharadwaj, Qsipchuk, Mease, and Park using a switched controller.²²

The proposed inverse optimal control laws are based on minimum norm optimization because of its interesting similarity with problems involving an optimization tradeoff between integrated torque and maneuver time. Indeed, both these problems are solved by switching between a zero torque mode, acceleration and deceleration modes. Minimum time is not reached by the min-norm law but the controller enhances settling time compared to a benchmark law and has the robustness advantages of feedback control. The min-norm law under consideration minimizes the norm of the torque, while imposing as a minimum the convergence

rate of a Lyapunov function under the nonlinear singular controller. The min-norm law is then modified by gain scheduling to incorporate realistic instantaneous torque constraints. The tradeoff between integrated torque and settling time is shown in section VI to be enhanced compared to the nonlinear singular controller, taken as a benchmark.

A first contribution of this paper compared to previous references is a stability proof, based on quaternion modeling, of 3-axis stability with two wheels by following desired singular angular velocity trajectories. A controller is proposed to follow these trajectories under zero momentum. This controller is tested in orbit. The second contribution is the angular velocity tracking controller approach, which is proven to stabilize the full state of a satellite using two wheels. The third contribution consists of a new inverse optimal controller for the underactuated satellite, which is shown to significantly enhance the settling time (given a level of integrated torque), compared to the snlc controller taken as a benchmark, particularly about the unactuated axis. This controller makes angular velocity tracking a viable approach and is potentially more efficient than the one already tested in-orbit.

The paper is organized as follows: The dynamic and kinematic models of the underactuated satellite are presented in section II. In section III, a specific angular velocity trajectory, consisting of nonlinear singular law is shown to stabilize the attitude of an underactuated satellite on all three axes using two wheels. In section IV, two approaches are proposed to generate this desired angular velocity trajectory. The first one is obtained from the perfect zero momentum assumption, while the other is based on angular velocity tracking. In section V, the min-norm inverse optimal approach^{21,22,24,25} is proposed to enhance the torque-rapidity tradeoff compared to the nonlinear singular controller, by only consuming torque in the phase space regions where convergence rate is locally enhanced.

Finally, a comparative numerical simulation analysis in section VI demonstrates the control performance enhancement by the inverse optimal controller (based on angular velocity tracking), compared to the 3-axis converging nonlinear singular controller used as a benchmark (based on a zero momentum condition or on angular velocity tracking). The three axis stabilization of an underactuated satellite with two wheels is demonstrated in-orbit using the nonlinear singular controller.

II. Dynamic and kinematic models

In the absence of external disturbance torques, the model of attitude dynamics is given by:

$$\dot{\mathbf{L}} + \boldsymbol{\omega} \times \mathbf{L} = 0 \tag{1}$$

where L represents the total angular momentum in the body frame and $\boldsymbol{\omega} = [\omega_1, \omega_2, \omega_3]^T$ denotes the angular velocity vector of the body frame with respect to the inertial frame, expressed in body coordinates.

The equation of the total angular momentum L is:

$$\mathbf{L} = \mathbf{I}\boldsymbol{\omega} + \mathbf{h} \quad (2)$$

where \mathbf{h} is the angular momentum vector of the wheels.

The dynamics equation reduces to:

$$\mathbf{I}\dot{\boldsymbol{\omega}} = -\boldsymbol{\omega} \times (\mathbf{I}\boldsymbol{\omega} + \mathbf{h}) + \mathbf{u} \quad (3)$$

where the control torque is $\mathbf{u} = -\dot{\mathbf{h}}$

Let's assume without loss of generality that an actuator has failed on the Z axis, leading to $N_3 = h_3 = 0$.

For our underactuated satellite case, the spacecraft is known to only be controllable by two wheels in the case of a zero total angular momentum mode,¹⁷ which implies zero initial momentum.

The zero total angular momentum condition is:

$$\mathbf{I}\boldsymbol{\omega} + \mathbf{h} = \mathbf{0}$$

On the unactuated axis, the above condition also implies that:

$$\omega_3 = 0.$$

On the actuated axes, the momentum of the wheels compensates the momentum of the satellite without wheels. By substituting \mathbf{L} from equation (2), into the equation (1), the general Euler's rotational equation for the underactuated satellite with two wheels is simply given by:

$$\begin{aligned} I_1\dot{\omega}_1 &= N_1 \\ I_2\dot{\omega}_2 &= N_2 \\ I_3\dot{\omega}_3 &= 0 \end{aligned} \quad (4)$$

where $\mathbf{I} = \text{diag}(I_1, I_2, I_3)$ is the moment of inertia matrix of the satellite and where $N_i = -\dot{h}_i, i = 1, 2$ are the control torques of the wheels on the actuated axes.

Note however that the zero momentum condition is not perfectly conserved under a standard numerical integration scheme such as the Runge-Kutta fourth order integrator. Equation (3) is therefore used in the numerical simulation section to take that error into consideration, while zero momentum is considered for all stability analysis.

Based on the quaternion parameterization of attitude kinematics, the kinematic model of a satellite is given by:

$$\begin{aligned}\dot{\mathbf{q}} &= -\frac{1}{2}\boldsymbol{\omega} \times \mathbf{q} + \frac{1}{2}q_4\boldsymbol{\omega} \\ \dot{q}_4 &= -\frac{1}{2}\boldsymbol{\omega}^T \mathbf{q}\end{aligned}\tag{5}$$

After substituting the zero momentum condition $\omega_3 = 0$, the kinematic model of the satellite reduces to:

$$\begin{aligned}\dot{q}_1 &= \frac{1}{2}q_4\omega_1 - \frac{1}{2}q_3\omega_2 \\ \dot{q}_2 &= \frac{1}{2}q_3\omega_1 + \frac{1}{2}q_4\omega_2 \\ \dot{q}_3 &= -\frac{1}{2}q_2\omega_1 + \frac{1}{2}q_1\omega_2 \\ \dot{q}_4 &= -\frac{1}{2}q_1\omega_1 - \frac{1}{2}q_2\omega_2\end{aligned}\tag{6}$$

where $\bar{\mathbf{q}} = [\mathbf{q}, q_4]^T$ is the attitude quaternion, $\mathbf{q} = [q_1, q_2, q_3]^T$ is the vector part of the quaternion and ω_1, ω_2 can be seen as virtual control inputs to the attitude kinematic equations. Note that, although the angular velocity is referenced with respect to the inertial frame to simplify mathematical analysis, the angular velocity in the local orbit frame and the associated local orbit referenced attitude were used to construct the feedback laws during in-orbit experiments. The angular velocity in the local orbit frame is $\boldsymbol{\omega}_o = \boldsymbol{\omega} - \mathbf{A}[0, -n, 0]^T$, where n is the mean motion and \mathbf{A} denotes the attitude matrix.

The quaternion representation of attitude kinematics is adopted in order to avoid any singularities due to the attitude parameterization.

III. The desired converging angular velocity trajectories

In the following, the kinematic control problem is considered to determine the angular velocity trajectories that will allow for a 3-axis stabilized attitude in equation (6).

A. The singular control law

A singular controller approach was proposed by Tsiotras,¹¹ followed by S.Kim and Y. Kim¹⁴ to address the problem of 3-axis attitude control with two pairs of thrusters, which was characterized by a different controllability condition than the two wheel system. In the case of the underactuated satellite with two wheels, a singular controller was previously considered¹⁵ but the attitude kinematics in that paper were based on the Rodrigues-Gibbs parameters, which are known to potentially cause singularities. A similar control law is therefore constructed here based on quaternion modeling:

$$\begin{aligned}\omega_{d1} &= -kq_1 + g \frac{q_2 q_3}{q_1^2 + q_2^2} \\ \omega_{d2} &= -kq_2 - g \frac{q_1 q_3}{q_1^2 + q_2^2}\end{aligned}\tag{7}$$

where the subscript ‘ d ’ stands for the desired value of the angular velocity.

In equation (7), the proportional part of the feedback controller is dedicated to the stabilization of the actuated axes, while the discontinuous or singular interconnection terms allow for the stabilization of the unactuated axis. This controller is therefore converging rather than stabilizing.

Note that equation (6) only represents a stepping stone towards the control of the full state vector. It can be seen as an inner loop controller, which cannot be implemented alone. Indeed, an outer loop controller is generally required in practice to control the attitude of the underactuated satellite.

For this closed loop system, singularities can be avoided because, the numerator will be shown to exponentially converge to zero faster than the denominator. However, in practice, as also proposed by Tsiotras and Doumchenko in the case of thrusters,¹¹ a saturated version of the proposed controller is required to avoid singularities, which are possible in practice in the presence of noise and other uncertainties.

$$\begin{aligned}\omega_{d1} &= -kq_1 + g \text{sat} \left(\frac{q_2 q_3}{q_1^2 + q_2^2}, a_1 \right) \\ \omega_{d2} &= -kq_2 - g \text{sat} \left(\frac{q_1 q_3}{q_1^2 + q_2^2}, a_2 \right)\end{aligned}\tag{8}$$

where a_1, a_2 are strictly positive and constant saturation limits.

B. Stability proof

Despite the fact that mathematical stability proofs are often made more complicated using this parameterization, the absence of singularities and the fact that quaternions are readily available in the onboard attitude control software of most satellites makes this parameterization more attractive than the Rodrigues/Gibbs parameters. A similar approach was also used by S.Kim and Y.Kim but the problem under consideration was the case of a pairs of thrusters. Also, the stability analysis in that paper was more complicated than necessary as the convergence rates of the full attitude had to be calculated.

By substituting the expressions of the virtual angular velocity inputs from equation (7) into equation (6), the closed loop dynamics on the unactuated axis are given by:

$$\dot{q}_3 = -\frac{g}{2}q_3\tag{9}$$

Therefore, the attitude component $q_3 = q_{30}e^{(-g/2)t}$ about the unactuated axis converges to zero. It remains to be shown that $q_1^2 + q_2^2$ also converges to zero.

The time derivative of q_4 is greater than zero for any nonsingular attitude:

$$\begin{aligned}
\dot{q}_4 &= -\frac{1}{2}q_1\omega_1 - \frac{1}{2}q_2\omega_2 \\
&= -\frac{1}{2}q_1 \left(-kq_1 + g\frac{q_2q_3}{q_1^2 + q_2^2} \right) - \frac{1}{2}q_2 \left(-kq_2 - g\frac{q_1q_3}{q_1^2 + q_2^2} \right) \\
&= \frac{1}{2}k(q_1^2 + q_2^2) \geq 0
\end{aligned} \tag{10}$$

From equation (10), the first obvious conclusion is that q_4 is an increasing monotonic function of time. The usual approach to proving stability is to use this information when differentiating $q_1^2 + q_2^2$, to prove that the attitude on the actuated axes converges to zero. This however makes proving stability more complicated than needed. It is indeed important to note that \dot{q}_4 is not only positive but also proportional to $q_1^2 + q_2^2$. Also, q_4 is an increasing and bounded function, therefore it converges when time goes to infinity. The convergence of q_4 implies the convergence \dot{q}_4 to 0, when time goes to infinity. From the specific expression of \dot{q}_4 , this also implies that $\lim_{t \rightarrow \infty} (q_1^2 + q_2^2) = 0$ and there is no need to differentiate $q_1^2 + q_2^2$ to reach that conclusion.

C. Singularity of the controller

The state vector $\mathbf{x} = [\bar{\mathbf{q}}, \boldsymbol{\omega}]$ is defined on the manifold

$$\Omega = \{(\bar{\mathbf{q}}, \boldsymbol{\omega}), q_1^2 + q_2^2 \neq 0\}.$$

The initial condition must therefore be chosen in the manifold Ω .

It can then be shown that whenever the initial condition belongs to the manifold Ω , the trajectories can be shown to never enter the singular state. This was shown by S.Kim and Y.Kim for a thruster control problem¹⁴ and a brief similar analysis is used here with two wheels. To this end, the variable $V_q(t) = q_1^2 + q_2^2$ is defined.

$$\begin{aligned}
\dot{V}_q &= -kq_4V_q(t) + gq_3^2(0)e^{-gt} \\
&< -kq_4(0)V_q(t) + gq_3^2(0)e^{-gt}
\end{aligned} \tag{11}$$

It is then possible to define a function $U(t)$ such that $U(0) = V_q(0)$ and $\dot{U} = -kq_4(0)U(t) + gq_3^2(0)e^{-gt}$. This differential equation has an analytic solution of the form $U(t) = ae^{-kq_4(0)t} + be^{-gt}$. After defining this function, equation (11) yields $\dot{V}_q + kq_4(0)V_q(t) < \dot{U} + kq_4(0)U(t)$ and since $q_4 > q_4(0)$, it follows that $\dot{V}_q(0) < \dot{U}(0)$ and $\dot{V}_q - \dot{U} < -kq_4(0)(V_q - U)$ meaning that $V_q(t)$ converges to $U(t)$ as time goes to infinity and both quantities approach zero. $U(t)$ has an analytical solution $U(t) = ae^{-kq_4(0)t} + be^{-gt} < ae^{-kt} + be^{-gt}$.

The singularity in the control law (7) can therefore be ruled out if $\frac{q_3}{q_1^2 + q_2^2}$ converges exponentially to zero whenever the initial attitude is nonsingular. As the system (and V_q) approaches the origin, $\frac{q_3}{q_1^2 + q_2^2} \rightarrow$

$\frac{q_3(0)e^{(-g/2)t}}{ae^{-kt} + be^{-gt}}$, and the numerator of the singular term converges faster to zero than the denominator whenever $g > 2k$.

IV. Full state control strategies for the underactuated satellite

In the previous section, an expression was derived for the required angular velocity commands to stabilize the attitude quaternions on all three axes. For the underactuated satellite, these angular velocity commands must be generated from two actuators, considered here to be reaction wheels.

Two possible ways of generating the desired trajectories are envisioned in the following subsections. First, it is assumed that the satellite is in a perfect zero momentum mode and the required control inputs are directly obtained from the zero momentum assumption. In the following subsection, a different approach is considered, based on angular velocity tracking by a proportional feedback law with compensation of nonlinear dynamics.

A. Control input generation from the zero momentum condition

The zero angular momentum assumption can be written as follows on the actuated axes:

$$\begin{aligned} I_1\omega_1 + h_1 &= 0 \iff h_1 = -I_1\omega_1 \\ I_2\omega_2 + h_2 &= 0 \iff h_2 = -I_2\omega_2 \end{aligned} \tag{12}$$

Equation (12) is always satisfied in a zero total angular momentum mode. Under a perfect zero momentum condition, the condition $\omega_i = \omega_{di}$, $i = 1, 2$ can easily be satisfied by applying the momentum wheel commands $h_i = -I_i\omega_{di}$ $i = 1, 2$ where ω_{di} is given by equation (7). The required wheel speed commands, under zero momentum, are then given by:

$$\begin{aligned} \dot{\theta}_1 &= -\frac{I_1}{I_{wh1}}\omega_{d1} \\ \dot{\theta}_2 &= -\frac{I_2}{I_{wh2}}\omega_{d2} \end{aligned} \tag{13}$$

where $\dot{\theta}_i$ is the i^{th} wheel speed and I_{whi} is the moment of inertia of the i^{th} wheel, with $i=1,2$.

The control torques can then be computed by differentiating the wheels momenta. This is only done for comparison purposes, since the wheel speed demand is the actual input sent to each wheel.

An important feature of this control approach is that the control input is an attitude only feedback, because the wheel speeds $\dot{\theta}_i$ are functions of ω_{di} , $i = 1, 2$, which only depend on the attitude. This is particularly suitable for applications requiring attitude control without angular velocity measurements, but this requires the zero total momentum condition to be satisfied perfectly (or almost perfectly in practice).

B. Attitude control by angular velocity tracking

A robust way of practically implementing the underactuated attitude control scheme is to consider the dynamic and kinematic models as a cascade system where the desired angular velocities are tracked to stabilise the attitude. Stability of the system is obtained from a passivity argument, which was previously described by Tsiotras et al, among other references.

1. Angular velocity tracking law

The control torque for the outer angular velocity tracking loop is proposed to simply consist of a proportional feedback law:

$$u_{snlci} = I_i(-K_i(\omega_i - \omega_{di}) + \dot{\omega}_{di}), i = 1, 2 \quad (14)$$

where ω_{di} is obtained from equation (7), K_i is a constant scalar gain and snlc stands for singular nonlinear controller. This controller achieves exponential convergence of the angular velocity to its desired value in the zero momentum case. Note that, although the last term may not be necessary in practice when the proportional gains are sufficiently high, this term makes stability easier to prove.

The following Lyapunov function can be used to prove stability of the full cascade system (dynamic and kinematic model) with the outer loop controller of equation (14) and inner loop controller of equation (7):

$$V = k(\mathbf{q}^T \mathbf{q} + (1 - q_4)^2) + \frac{1}{2}(\boldsymbol{\omega} - \boldsymbol{\omega}_d)^T(\boldsymbol{\omega} - \boldsymbol{\omega}_d) \quad (15)$$

Note that, under the zero momentum controllability condition, the third components of the vectors $\boldsymbol{\omega}, \boldsymbol{\omega}_d$ are zero with $\boldsymbol{\omega}_d = [\omega_{d1}, \omega_{d2}, 0]^T$ are zero.

2. Stability proof for the cascade system

The Lyapunov function V can be constructed using a backstepping approach, where the reduced Lyapunov function

$$V_1 = k(\mathbf{q}^T \mathbf{q} + (1 - q_4)^2) = 2k(1 - q_4)$$

is used in a first instance to prove stability of the kinematic model using the angular velocity $\boldsymbol{\omega}_d$ from equation (8) as a virtual control input. Indeed V_1 is positive and from section III.B, it can also be concluded that V_1 is decreasing. For simplicity, it is assumed that $q_4 = 1$ is the desired equilibrium where V_1 is zero, although the equilibrium $q_4 = -1$, corresponding to the same physical orientation, can also be obtained through a slight modification of the control law as shown by Bong Wie.²⁶

Following the backstepping design procedure, the Lyapunov function V can be obtained by adding the

deviation with respect to the virtual control input to V_1 :

$$\begin{aligned} V &= V_1 + \frac{1}{2}(\boldsymbol{\omega} - \boldsymbol{\omega}_d)^T(\boldsymbol{\omega} - \boldsymbol{\omega}_d) \\ &= 2k(1 - q_4) + \frac{1}{2}(\boldsymbol{\omega} - \boldsymbol{\omega}_d)^T(\boldsymbol{\omega} - \boldsymbol{\omega}_d) \end{aligned} \quad (16)$$

Note that, with $k > 0$, $V > 0, \forall x \in \Omega$.

The time derivative of the Lyapunov function V , constructed using a backstepping approach, is given by:

$$\dot{V} = -2k\frac{k}{2}(q_1^2 + q_2^2) + (\boldsymbol{\omega} - \boldsymbol{\omega}_d)^T(\dot{\boldsymbol{\omega}} - \dot{\boldsymbol{\omega}}_d) \quad (17)$$

$$\dot{V} = -k^2(q_1^2 + q_2^2) + (\boldsymbol{\omega} - \boldsymbol{\omega}_d)^T(-\mathbf{I}^{-1}\boldsymbol{\omega} \times (\mathbf{I}\boldsymbol{\omega} + \mathbf{h}) - \mathbf{K}(\boldsymbol{\omega} - \boldsymbol{\omega}_d)) \quad (18)$$

where $\mathbf{K} = \text{diag}(K_1, K_2)$.

Under the assumption of a zero momentum satellite $\|\mathbf{I}\boldsymbol{\omega} + \mathbf{h}\| = 0$, representing to the controllability condition with two wheels, equation (18) reduces to:

$$\dot{V} = -k^2(q_1^2 + q_2^2) - (\boldsymbol{\omega} - \boldsymbol{\omega}_d)^T \mathbf{K}(\boldsymbol{\omega} - \boldsymbol{\omega}_d) \quad (19)$$

From equation (19), $\dot{V} < 0, \forall \mathbf{x} \in \Omega$ stability is guaranteed.

Note that this condition is satisfied for a zero momentum satellite $\|\mathbf{I}\boldsymbol{\omega} + \mathbf{h}\| = \mathbf{0}$.

The proposed function V therefore decreases by making $K_1 > 0, K_2 > 0$ (The first term in \dot{V} was obtained assuming k, g positive). Lasalle's invariance principle²⁹ can then be used to show that the singular origin is approached when $V \rightarrow 0$ since $\boldsymbol{\omega}_d$ is then tracked and $q_4 \rightarrow 1$ also implying that $\boldsymbol{\omega} \rightarrow \mathbf{0}$. Also, from III.c, the system does not enter a singular state in this noise and disturbance free case.

Using the saturated version of the singular control law, the interconnection terms are bounded and stability would still be obtained but when $\boldsymbol{\omega}_d$ is tracked, the final state does not necessarily approach zero. Numerical simulations suggest that a limit cycle is then obtained at a neighborhood of the origin, of which the amplitude depends on the saturation limit. It is however technically possible to ensure that $[\mathbf{q}, q_4, \boldsymbol{\omega}]^T = [0_{3 \times 1}, \pm 1, 0_{3 \times 1}]^T$ is an equilibrium point of the system. This is done by replacing the denominator of equation (7) by $q_1^2 + q_2^2 + \epsilon$, where ϵ is a small positive constant. That was necessary for in-orbit testing.

V. Inverse optimal attitude control of the underactuated satellite

In the numerical simulation section, the full state nonlinear singular controller of equation (14) based on the angular velocity tracking approach will be shown to be less efficient, in terms of settling time for a

level of the integrated torque, than the singular controller of equation (13) derived from the zero momentum condition, with attitude only feedback .

However, the advantage of the angular velocity tracking approach is that it can be modified and potentially enhanced. Inverse optimal control theory is used in this section to enhance the performance of the full state feedback controller of equation (13). The proposed inverse optimal control approach is based on the design of phase space trajectories, and is therefore not applicable to the controller of equation (13) with attitude feedback only.

For the sake of convenience, the inverse optimal control problem is formulated by representing our system of equations (3) and (6) as an affine control system of the form:

$$\begin{aligned}\dot{\mathbf{x}} &= f(\mathbf{x}, \mathbf{h}) + g(\mathbf{x})\mathbf{u} \\ \dot{\mathbf{h}} &= -\mathbf{u}\end{aligned}\tag{20}$$

where:

$$\begin{aligned}\mathbf{x} &= [\bar{\mathbf{q}}, \boldsymbol{\omega}]^T \\ \mathbf{u} &= [N_1, N_2, 0]^T \\ f(\mathbf{x}, \mathbf{h}) &= [\dot{\bar{\mathbf{q}}}, \dot{\boldsymbol{\omega}}]_{\mathbf{u}=\mathbf{0}_{3 \times 1}}^T \\ g(\mathbf{x}) &= \begin{bmatrix} \mathbf{0}_{4 \times 3} \\ \mathbf{I}^{-1}_{3 \times 3} \end{bmatrix}^T\end{aligned}$$

and the variables N_1, N_2 respectively represent the control torques of the wheels mounted on the X and Y body axes of the satellite.

The zero momentum condition is used for stability analysis, but not enforced in numerical simulations where momentum is initialized at zero and the controller is shown to work under numerical integration errors that do not perfectly conserve angular momentum.

Inverse optimal control design starts from the construction of a converging control law, known as the benchmark controller, with respect to a so-called Control Lyapunov Function (CLF) V . For a CLF, there exists by definition a control input u satisfying:

$$L_f V(\mathbf{x}, \mathbf{h}) + L_g V(\mathbf{x})\mathbf{u}(\mathbf{x}) < 0\tag{21}$$

where the Lie derivatives are defined as $L_g V = \frac{\partial V^T}{\partial \mathbf{x}} g$ and $L_f V = \frac{\partial V^T}{\partial \mathbf{x}} f$

However, \mathbf{u} is not unique in general. Inverse optimal construction is a way of determining a specific but optimal stabilizing control input.

In inverse optimality, the cost function is not directly specified, and the optimization problem is often posed as a nonlinear program. The system can then be shown to be optimal (solve a Hamilton Jacobi Bellman equation) with respect to a meaningful cost function.²⁵

A. Standard Minimum Norm Control

A particularly interesting nonlinear control construction based on the existence of a Control Lyapunov function is the minimum-norm control law proposed by Freeman and Kokotovic.²⁵

This approach was applied to the attitude control of a satellite.^{22,27}

The minimum norm pointwise optimization problem is posed as follows:

$$\text{Minimize } \|\mathbf{u}\| \quad \text{st.} \quad \dot{V}_{\mathbf{u}} \leq \dot{V}_{\mathbf{k}(\mathbf{x})} \quad (22)$$

The above minimum-norm control problem is the pointwise optimization problem of minimizing the control effort subject to a constraint on the convergence rate of the CLF V . The optimization constraint is that the time derivative of V under the effect of a benchmark controller $\mathbf{k}(\mathbf{x})$ is imposed as a minimum convergence rate. Note that the optimization constraint can also be seen as a Hamilton-Jacobi-Bellman (HJB) inequality.²¹

It was shown by Kokotovic et al.²¹ that this controller solves an optimal tradeoff between torque expenditure and rapidity by minimizing a meaningful cost function of the form

$$J = \int_0^{\infty} \{l(\mathbf{x}) + r(\mathbf{x}, \mathbf{u})\} dt \quad (23)$$

where $l(\mathbf{x})$ is a continuous positive definite function of \mathbf{x} and $r(\mathbf{x}, \mathbf{u})$ is positive definite increasing convex function of \mathbf{x} and a norm of \mathbf{u} . Also note that the fact that an optimization trade-off is being achieved is evident from the nonlinear program stated in equation (13), which is solved analytically. Indeed, a norm of the torque is minimized subject to a rapidity constraint, which represents the other side of the trade-off.

The minimum-norm nonlinear program can be solved analytically.

1. *Benchmark controller*

As a benchmark controller $\mathbf{k}(\mathbf{x})$ to be enhanced for the underactuated satellite, the control law of equation (14) based on the angular velocity tracking approach, is considered. It is again written here for clarity:

$$\mathbf{k}(\mathbf{x}) = \mathbf{u}_{snlc} = -\mathbf{I}_r(\mathbf{K}_m(\boldsymbol{\omega} - \boldsymbol{\omega}_d) - \dot{\boldsymbol{\omega}}_d) \quad (24)$$

where $\mathbf{K} = \text{diag}(K_1, K_2)$, $\mathbf{I}_r = \text{diag}(I_1, I_2)$.

2. *Standard Min-norm control law*

The switching condition in equation (22) can also be written as a function of $L_g V$ because:

$$\dot{V} - \dot{V}_{\mathbf{k}(\mathbf{x})} = (L_f V + L_g V \mathbf{u}) - (L_f V + L_g V \mathbf{k}(\mathbf{x})) = L_g V (\mathbf{u} - \mathbf{k}(\mathbf{x}))$$

The benchmark controller $\mathbf{k}(\mathbf{x})$ is enhanced by minimum norm optimization because the norm of the torque is minimized under the convergence rate constraint with the benchmark law.

The minimum norm problem of equation (22) was solved in the literature.^{21,22} The optimization inequality constraint of equation (22) can also be written as $L_g V \mathbf{u} \leq L_g V \mathbf{k}(\mathbf{x})$. When $L_g V \mathbf{k}(\mathbf{x}) \geq 0$, then the control input of minimum norm that solves this constraint is simply $\mathbf{u}_{opt} = \mathbf{0}$. This allows for a more efficient use of control effort. In fact, applying the benchmark law in the region where $L_g V \mathbf{k}(\mathbf{x}) \geq 0$ would slow down the response at any point \mathbf{x} by decreasing the negativity of \dot{V} . Otherwise, when $L_g V \mathbf{k}(\mathbf{x}) < 0$ then the solution \mathbf{u}_{opt} of minimum norm is the same as the minimum norm solution subject to the equality constraint $L_g V \mathbf{u} = L_g V \mathbf{k}(\mathbf{x})$, which is known to be a projection in the direction of the vector $L_g V^T$ and such that $\|\mathbf{u}\| = \|\mathbf{k}(\mathbf{x})\|$. More explicitly, the minimum norm control law that solves the optimization problem of equation (22), under the benchmark controller of equation (24), is given by:

$$\mathbf{u}_{opt} = \begin{cases} -\frac{(L_g V \mathbf{u}_{snlc})(L_g V)^T}{L_g V (L_g V)^T} & \text{if } L_g V \mathbf{u}_{snlc} < 0 \\ 0 & \text{if } L_g V \mathbf{u}_{snlc} \geq 0 \end{cases} \quad (25)$$

where the term $L_g V \mathbf{u}_{snlc}$ is a scalar and the projection is in the direction of $L_g V^T$. In the numerical simulation study, the following parameterized Lyapunov function will be used:

$$V = k(\mathbf{q}^T \mathbf{q} + (1 - q_4)^2) + \frac{1}{2}(\boldsymbol{\omega} - \boldsymbol{\omega}_{\gamma,\sigma})^T (\boldsymbol{\omega} - \boldsymbol{\omega}_{\gamma,\sigma}) \quad (26)$$

where $\boldsymbol{\omega}_{\gamma,\sigma}$ is given by:

$$\begin{aligned}\omega_{1(\gamma,\sigma)} &= -\gamma q_1 + \sigma \text{sat}\left(\frac{q_2 q_3}{q_1^2 + q_2^2}, a_1\right) \\ \omega_{2(\gamma,\sigma)} &= -\gamma q_2 - \sigma \text{sat}\left(\frac{q_1 q_3}{q_1^2 + q_2^2}, a_2\right)\end{aligned}\tag{27}$$

where $\gamma < k, \sigma < g$ are positive constants.

Note that the proposed Lyapunov function is similar to the one constructed by backstepping in section IV.B.2, the difference being that the parameters γ and σ are now introduced to allow for the tuning of the min-norm controller, which explicitly depends on V . The phase space region where the zero torque mode can then be adjusted by varying those parameters. The switching function $L_g V^T = 0 \Rightarrow \omega - \omega_{\gamma,\sigma} = 0$, where the controller is typically turned off, is then given by a curve which consists of the sum of a straight line with the singular interconnection term. The other switching curve, where the controller is typically reactivated, is $\mathbf{u}_{snlc} = \mathbf{0}$, which also represents the sum of a linear term and a nonlinear singular contribution. The control torque is also turned off when the vectors $L_g V, \mathbf{u}_{snlc}$ are orthogonal, but this is less likely in practice when γ and σ are respectively sufficiently smaller than k and g .

3. Stability conditions under min-norm control

Following a Lyapunov approach similar to the one in section IV.B.2, the new parameterized expression of V from equation (26) will be proven to be a Lyapunov function under the benchmark controller $\mathbf{k}(\mathbf{x})$, which is sufficient for the stability of the system by minimum norm control, given the optimization constraint in equation (22).

Positivity of V : The condition on the positivity of V is satisfied whenever $\boldsymbol{\omega} \neq \boldsymbol{\omega}_{\gamma,\sigma}$ and $[\mathbf{q}, q_4] \neq [0, 0, 0, \pm 1]$.

The term $\omega_{\gamma,\sigma}$ of the Lyapunov function is not defined at the point $[\mathbf{q}, q_4] = [0, 0, 0, \pm 1]$, but, as argued earlier, it converges to zero when the system approaches that equilibrium point because the denominator of the singular term converges to zero before the numerator.

Negativity of \dot{V} : For simplicity, the unsaturated version of equation (27) is considered. The time derivative of V is then given by:

$$\dot{V} = -2k \frac{k}{2} (q_1^2 + q_2^2) + (\boldsymbol{\omega} - \boldsymbol{\omega}_{\gamma,\sigma})^T (\dot{\boldsymbol{\omega}} - \dot{\boldsymbol{\omega}}_{\gamma,\sigma})\tag{28}$$

$$\dot{V} = -k^2 (q_1^2 + q_2^2) - (\boldsymbol{\omega} - \boldsymbol{\omega}_{\gamma,\sigma})^T \mathbf{K} (\boldsymbol{\omega} - \boldsymbol{\omega}_{\gamma,\sigma})\tag{29}$$

In a zero momentum mode (which is assumed because it is a controllability condition with two wheels), the expression of \dot{V} simplifies to : $\dot{V} = -k^2 (q_1^2 + q_2^2) - (\boldsymbol{\omega} - \boldsymbol{\omega}_{\gamma,\sigma})^T \mathbf{K} (\boldsymbol{\omega} - \boldsymbol{\omega}_{\gamma,\sigma})$ and is negative with

$K_1 > 0, K_2 > 0$ where $\mathbf{K} = \text{diag}(K_1, K_2)$, (k, g must also be positive for the first term of \dot{V} to be valid) and to ensure attitude convergence to zero. As in section IV.B.2, Lasalle's invariance principle can be used to show convergence to the singular origin (without reaching the singular state for reasons mentioned in III.c) when the angular velocity is tracked. However, using the saturated version of the control law, when $\omega_{\gamma, \sigma}$ is tracked, it is conjectured that the final states do not necessarily converge to zero but to a neighborhood of zero.

The minimum norm controller achieves an inverse optimal tradeoff between control effort and convergence rate.²¹ A min-norm controller may be allowed higher gains to achieve a faster response while consuming the same overall torque as a benchmark controller with lower gains. The issue with this approach is that instantaneous torque limitations are not taken into consideration in the controller switching logic because the same gains are used everywhere when the controller is activated, potentially causing torque saturation.

B. Gain scheduled min-norm law

The control law of equation (25) achieves an enhancement of the torque-rapidity tradeoff compared to the benchmark controller, but it was shown in a previous paper that, using the same gains as the benchmark law, the torque expenditure can only be significantly reduced at the expense of a slightly slower response.²⁴ In that paper, the standard min-norm law was then tuned using higher gains to deliver the same integrated torque as the benchmark law and settling time was reduced. However, a new issue arose because the maximum instantaneous torque reached during the maneuver increased significantly, potentially causing torque saturation. This is due to the fact that standard min norm law does not incorporate torque saturation limits. This problem was then solved by a gain scheduled version of the minimum norm control law,^{24, 28} where apart from the zero torque mode (still obtained from standard min-norm theory), higher gains are used whenever there are no torque saturation issues to favor rapidity, and lower gains are used otherwise. The gain scheduled control law that was developed in those papers was designed for a fully actuated satellite. A very similar gain scheduling logic is proposed here for the underactuated satellite:

$$\mathbf{u}_{opt} = \begin{cases} \frac{(L_g V \mathbf{u}_{lg})(L_g V)^T}{L_g V (L_g V)^T} & \text{if } L_g V \mathbf{u}_{hg} < 0 \quad \text{and} \quad \|\mathbf{u}_{hg}\|_\infty \geq \epsilon \\ 0 & \text{if } L_g V \mathbf{u}_{hg} \geq 0 \\ \frac{(L_g V \mathbf{u}_{hg})(L_g V)^T}{L_g V (L_g V)^T} & \text{if } L_g V \mathbf{u}_{hg} < 0 \quad \text{and} \quad \|\mathbf{u}_{hg}\|_\infty < \epsilon \end{cases} \quad (30)$$

where ϵ is a positive constant, typically a fraction of the torque saturation limit, the subscripts lg and hg respectively stand for low gain mode and high gain mode and the components of the low gain law \mathbf{u}_{lg} on the

actuated axes are:

$$\begin{aligned} u_{lg1} &= -K_1 \left(\omega_1 + k_1 q_1 - g_1 \text{sat} \left(\frac{q_2 q_3}{q_1^2 + q_2^2}, a_1 \right) \right) + I_1 \dot{\omega}_{d1} \\ u_{lg2} &= -K_1 \left(\omega_2 + k_1 q_2 + g_1 \text{sat} \left(\frac{q_1 q_3}{q_1^2 + q_2^2}, a_2 \right) \right) + I_2 \dot{\omega}_{d2} \end{aligned} \quad (31)$$

The gains of the low gain mode are those of the benchmark *snlc* singular controller to be enhanced from equations (24) and (8). In the phase space region where there are no torque saturation constraints, it is then possible to make use of the high gain mode, without increasing the integrated torque compared to the benchmark controller, because the torque is turned off during part of the manoeuvre. The high gain law \mathbf{u}_{hg} has the components:

$$\begin{aligned} u_{hg1} &= -K_2 \left(\omega_1 + k_2 q_1 - g_2 \text{sat} \left(\frac{q_2 q_3}{q_1^2 + q_2^2}, a_1 \right) \right) + I_1 \dot{\omega}_{d1} \\ u_{hg2} &= -K_2 \left(\omega_2 + k_2 q_2 + g_2 \text{sat} \left(\frac{q_2 q_3}{q_1^2 + q_2^2}, a_2 \right) \right) + I_2 \dot{\omega}_{d2} \end{aligned} \quad (32)$$

where the gains are chosen such that: $k_2 > k_1, g_2 > g_1, K_2 > K_1$.

Note that the stability of the system by gain scheduled min-norm control is satisfied when both the low gain and high gain modes stabilize the system. The stability proof is then a consequence of previous proofs. Indeed, the gain scheduled min-norm controller solves the optimization problem:

$$\text{Minimise } \|\mathbf{u}\| \quad \text{st.} \quad \begin{cases} \dot{V} < \dot{V}_{\mathbf{u}_{hg}} & \text{if } \|\mathbf{u}_{hg}\|_\infty < \epsilon \\ \dot{V} < \dot{V}_{\mathbf{u}_{lg}} & \text{if } \|\mathbf{u}_{hg}\|_\infty \geq \epsilon \end{cases} \quad (33)$$

and stability follows when both $\dot{V}_{\mathbf{u}_{lg}}$ and $\dot{V}_{\mathbf{u}_{hg}}$ are negative. Higher gains tend to enhance the stabilization rate at the expense of torque expenditure, but as previously stated, the overall torque does not necessarily increase using the min-norm scheme because the size of the region where the controller is activated is typically reduced by increasing those gains, while keeping γ and σ fixed.

This gain scheduled min-norm controller will be shown to outperform the benchmark *snlc* controller by making the phase space trajectories of the system proceed more directly towards the origin (with less oscillations). This feature was also demonstrated in previous references,^{22,27} but is particularly significant in the case of the underactuated satellite, where the efficient tuning (with few transient oscillations) of the *snlc* controller can be particularly difficult to achieve in practice (compared to the tuning of a fully actuated satellite) using the required saturated version of the controller. Using gain scheduled min-norm optimization, efficient control is shown to be feasible, even in the typical situation when the benchmark controller cannot be efficiently tuned for our nonlinear system.

VI. Numerical simulations and in-orbit experiments

This section is divided into two subsections. The first subsection presents a numerical simulation analysis of the nonlinear singular controller and the proposed inverse optimal controller. The second subsection presents a practical in-orbit demonstration of 3-axis control by two control torques using the nonlinear singular controller.

The nonlinear singular controller was chosen for in-orbit testing to make practical implementation simpler when a first opportunity to test control algorithms in-orbit arose. These practical results also aim to justify further research on the implementation of underactuated attitude control. The proposed inverse optimal controller is shown in the numerical simulation section to be more advanced than the in-orbit tested singular controller. This controller is therefore seen as a candidate for future in-orbit implementation, when a new opportunity arises for in-orbit tests on the satellite Nigeriasat-X (Surrey Satellite Technology Limited (SSTL) platform), to be launched this year.

A. Numerical simulations

The parameters of the 320 kg mini-satellite Uosat-12 equipped with three reaction wheels, are considered in this numerical simulation section.

The moments of inertia of the principal axes are:

$$I_1 = 40.45, I_2 = 42.09, I_3 = 42.36(kg.m^2)$$

The attitude maneuver under consideration is a rest to rest maneuver from the initial condition:

$$q_1(0) = 0.2, q_2(0) = 0.2, q_3(0) = 0.2, q_4(0) = 0.8246$$

The controller gains of the snlc controller were: $k = 0.02rad/s$, $g = 0.08rad/sec$, $K_1 = K_2 = 10Nm.s/rad$. The controller gains of the gain scheduled min-norm controller were $k_1 = 0.02rad/sec$, $g_1 = 0.08rad/sec$, $k_2 = 0.2rad/sec$, $g_2 = 1.2rad/sec$, $K_1 = K_2 = 10Nm.s/rad$, $\epsilon = 0.02$, $a_1 = a_2 = 0.025$, $\gamma = 0.01rad/s$, $\sigma = 0.04rad/s$.

The torque saturation limit of the available reaction wheels in 20 milli Nm, but some simulations also assume a more capable reaction wheel with saturation levels of up to 100 milli Nm, which is realistic for SSTL's future mini-satellites.

In these simulations, the satellite is first controlled with all three wheels to an off-pointing attitude of 20 degrees on all three axes before being controlled by two wheels only (The 2 wheel mode is activated at time $t_0 = 500$ sec). This particular scenario stems from the fact that future planned underactuated

two wheels control experiments will not necessarily be tested on satellites with only two wheels following a wheel failure. The snlc controller is then used using the two proposed schemes: the one based on a zero momentum assumption and the one based angular velocity tracking. The snlc controller is then compared to the proposed gain scheduled min-norm controller, based on an snlc benchmark.

The integrated torque metric is $\int_{t_0}^{t_f} \sqrt{\mathbf{u}^T(t)\mathbf{u}(t)} dt$.

A low earth circular orbit at 600 km altitude was assumed for the target spacecraft, which corresponds to an orbital period of approximately 100 minutes.

Figures (1) and (2) show the torque profile and attitude response with two reaction wheels using the controller based on the zero momentum restriction of equation (13). The attitude is stabilized on all three axes with admissible torque. Further simulations (not shown here) have shown that improving the attitude response on the unactuated axis is possible at the expense of the response on the other two axes and that the sampling time (1 second here) cannot be allowed to exceed 5 seconds.

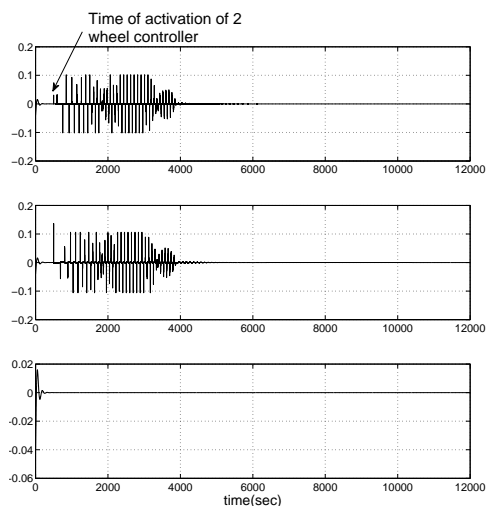


Figure 1. Control torque using the zero momentum restricted approach

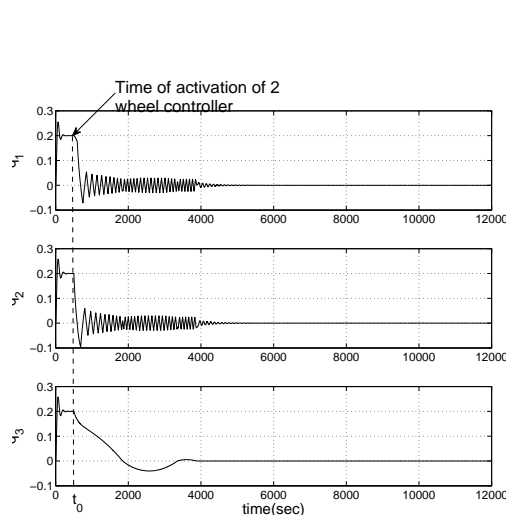


Figure 2. Attitude response using the zero momentum restricted approach

The control torque profile and the attitude response of the angular velocity tracking controller of equation (24) are respectively shown in figures (3) and (4). The attitude response is very slow for a level of the integrated torque (19.62 Nms), which was slightly higher than that of the zero momentum restricted approach (19.2 Nms). A faster response would require a much higher integrated torque to track the angular velocity trajectories more closely. The angular velocity tracking controller of equation (24) is therefore less efficient compared to the controller based on the exact zero momentum restriction.

The control torque profile and the attitude response of the gain scheduled min-norm controller of equation (30) are shown in figures (5) and (6). The attitude response is considerably enhanced compared to the snlc tracking controller of equation (24), and also compared to the zero momentum controller of equation (13),

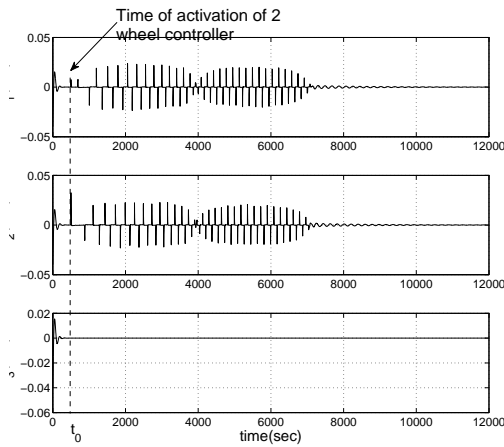


Figure 3. Control torque using the continuous angular velocity tracking approach

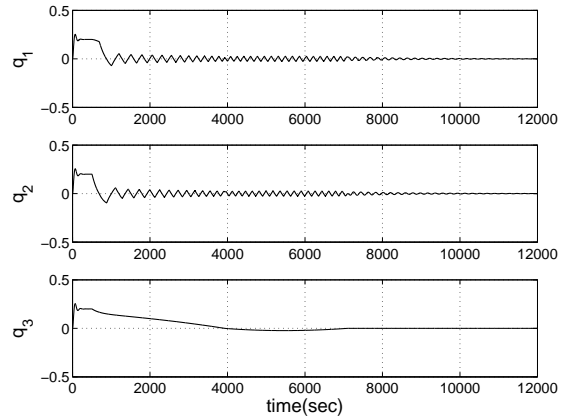


Figure 4. Attitude response using the continuous angular velocity tracking controller

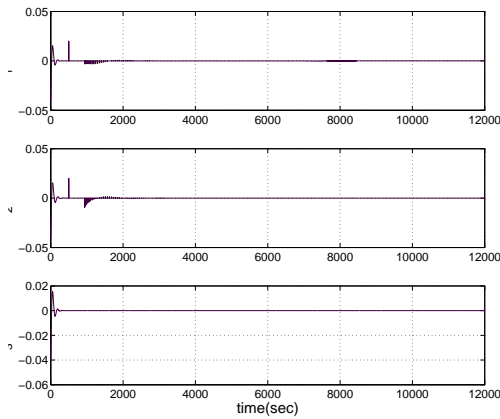


Figure 5. Control torque using the minimum-norm optimized angular velocity tracking approach

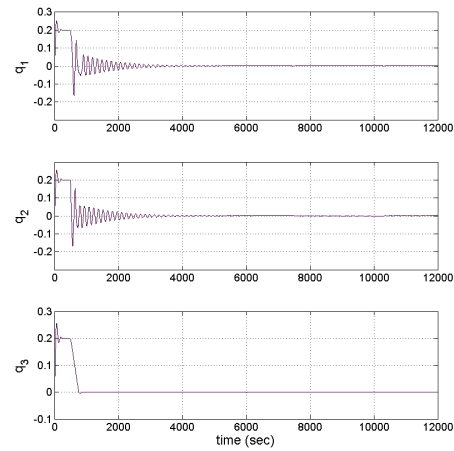


Figure 6. Attitude response using the minimum-norm optimized angular velocity tracking controller

despite a lower level of the integrated torque of 9.84 Nms, compared to 19.62 Nms.

The attitude response of all three controllers is compared on figure (7), where the off-pointing is characterised by the error on q_4 , which has the desired value $q_{4eq} = 1$. The settling time within 1 ± 0.02 (corresponding to attitude errors of approximately 0.5 degree) from the time t_0 when the underactuated mode is activated is: 521.5 sec with the gain scheduled min-norm controller, against 2452.1 sec with the zero momentum approach and 2918.8 sec with the snlc controller. These settling times are respectively increased to 1748.4 sec, 2956.5 sec and 7072.9 sec to settle within a finer error tolerance of 1 ± 0.01 . In this fine pointing case, the gain scheduled min-norm law based on angular velocity tracking reduces settling time by 41 percent.

Note that the attitude response with the gain scheduled min-norm controller allows for particularly

fast maneuvers on the unactuated axis, where the torques of two wheels are applied to stabilize that axis. This is an advantage of the two wheel controller compared to the alternative of using magnetic torquing to complement the wheels, as this would comparatively lead to a very limited rapidity on the unactuated axis. Yaw slew rate is enhanced without degrading the slew rate on other axes.

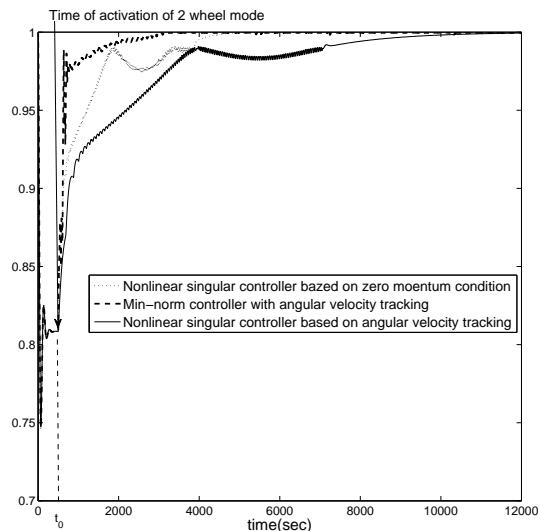


Figure 7. Attitude off-pointing using the snlc controllers and the PMN controller (Perfect when $q_4 = 1$)

The phase space trajectories of the gain scheduled min norm controller of equation (30), compared to the controller of equation (24) taken as a benchmark, are shown in figures (9) and (8) respectively. The initial maneuver to initialize the satellite at an off-pointing attitude because underactuated control is the same in both cases. When the underactuated law is activated, these figures show that the attitude overshoot on the unactuated axis q_3 is suppressed by the min-norm controller, which proceeds with less high frequency transient oscillations towards the origin's neighborhood (in 3D) and remains stable despite several horizontal zero torque phases. In certain phase space regions, the continuous controller consumes torque to unnecessarily slow the system down. The minimum norm controller achieves a more efficient tradeoff between settling time and torque expenditure. Note that due to the non geometric numerical integration scheme, ω_3 is not perfectly zero during the maneuver.

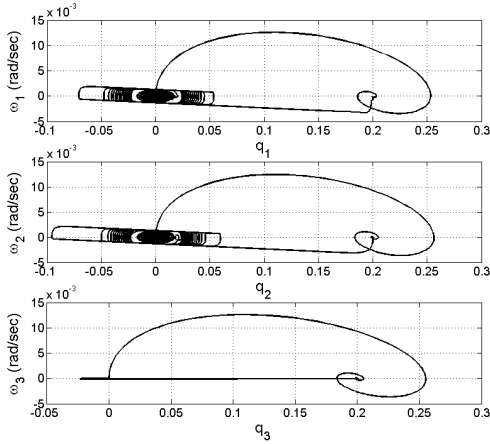


Figure 8. Phase space trajectory using the continuous snlc angular velocity tracking controller

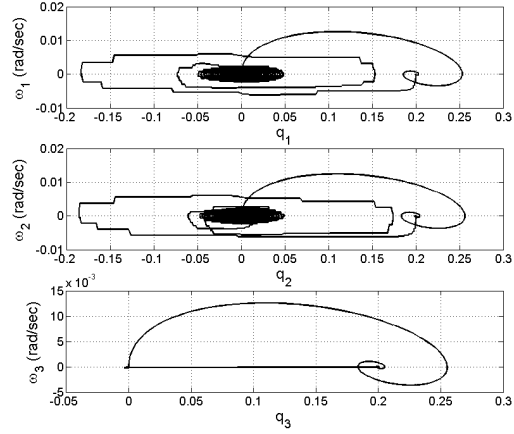


Figure 9. Phase space trajectory using the minimum-norm optimized angular velocity tracking approach

B. In orbit experiments

To demonstrate the feasibility of 3-axis attitude stabilization by two control torques and justify the practical motivation for studying this problem, two in-orbit experiments on Uosat-12 and UK-DMC1 are presented here. In these experiments, magnetic torquing was used prior to the activation of the underactuated controller with two wheels and a small bias momentum of -60 RPM had to be maintained on the Y-wheel for safety considerations. The telemetry of both satellites did not incorporate error covariance information. It is however known from sensor hardware characteristics that, in the case of Uosat-12, the attitude knowledge was of ± 0.2 degree, while the angular velocity knowledge is accurate within ± 0.025 degrees/sec. The maximum feasible wheel speed of Uosat-12 was 5000 RPM, while the maximum torque was 0.02 Nm and the sampling time was 10 seconds.

The first implementation of the snlc undeactuated controller of equations (7) and (13) was a sun tracking experiment on Uosat-12 with two wheels (because the Z-yaw wheel had failed). The gains were selected to be $k = 0.02, g = 0.06$ and the zero momentum condition was used to derive wheel speed commands. Figure (10) shows that the attitude on the unactuated axis was initially disturbed at the time of activation of the underactuated controller. The wheel speeds are those in figure (11). There was a tradeoff to achieve between the rapidity of the attitude response on the unactuated axis and the tracking performance on the actuated axes. Clearly, the tracking of the roll and pitch trajectories was not perfect in the underactuated control mode. However, the possibility of controlling the unactuated axis within bounded errors was demonstrated by this first experiment. The sun tracking experiment has shown a limited but existing control capability on all three axes using two wheels.

The second experiment of this paper was conducted to demonstrate the possibility of nadir pointing using

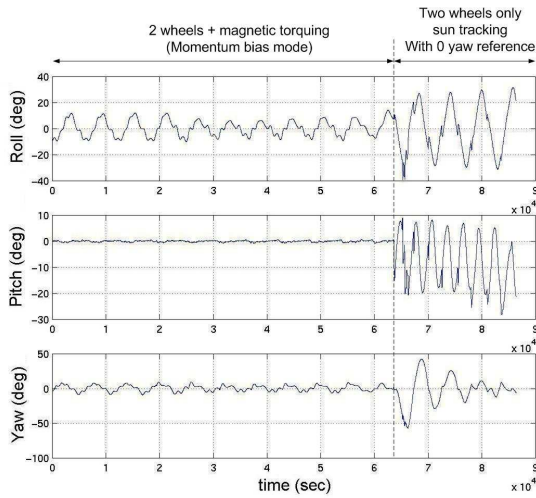


Figure 10. Attitude history during initial experimentation of sun tracking on Uosat-12 using two wheels

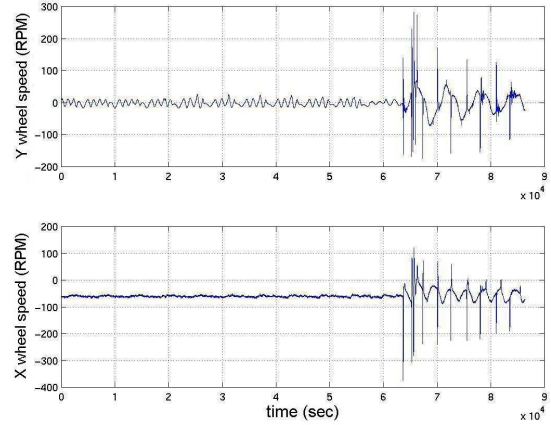


Figure 11. Wheel speeds of Uosat-12 using two wheels with, then without magnetic torquing on the unactuated axis

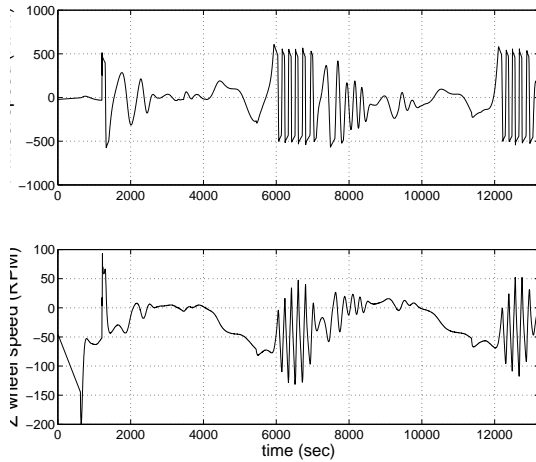


Figure 12. Wheel speeds recorded on the UK-DMC satellite using the zero momentum restricted singular controller

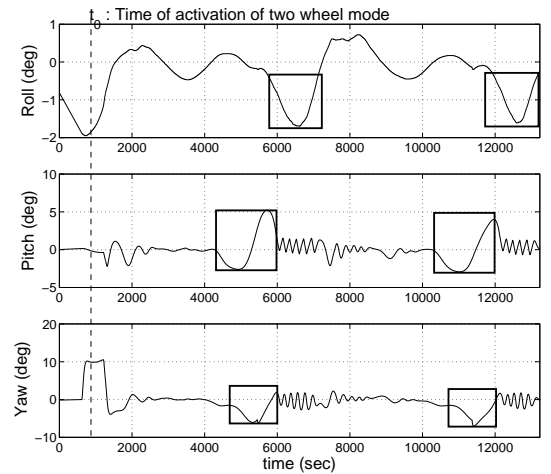


Figure 13. Attitude history of the underactuated UK-DMC satellite during two orbits using the zero momentum restricted singular controller

only two wheels onboard UK-DMC1 and zero magnetic torquing. The two wheels had a maximum torque capability of 0.01 Nm and a maximum wheel speed of 5000 RPM. The sampling time was 5 seconds. The attitude knowledge was 0.1 degree and the angular velocity knowledge was of 0.01 degrees per second. Note that UK-DMC1 was only equipped with two wheels (on the Y-pitch and Z-yaw axes) and had a gravity gradient boom deployed. However, the gravity gradient torque can only be seen as a disturbance, with no stabilizing effect under the underactuated singular controller with two wheels. The snlc controller was applied with the gains $k = 0.01$, $g = 0.05$, by taking subscripts 1, 2 and 3 in the control law of equation (8) to respectively represent the Y, Z and X axes. Before activating the underactuated controller for two orbits, magnetic torquing was used to complement the wheels and produce a satellite off-pointing of 10 degrees on

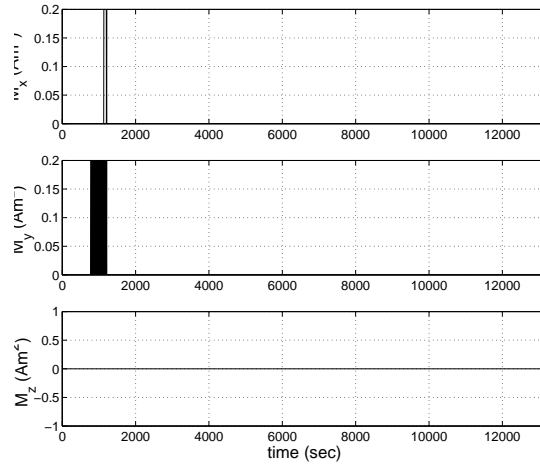


Figure 14. Magnetic dipole moment during UK-DMC experiment

the actuated yaw axis and 1.8 degree on the unactuated roll axis. A small 100 RPM momentum bias had to be imposed on the actuated Z axis for safety considerations, so the total momentum was not perfectly zero. Figure (12) shows the wheel speeds of the two available wheels of the micro-satellite UK-DMC1 using the controller of equations (13) and (8). In the underactuated control mode, the wheel speed was admissible during the initial maneuver. After the maneuver, the wheel speeds were pseudo periodic to counteract periodic disturbances. The control input is expectedly larger on the axis with higher moment of inertia.

The attitude response on all three axes during two orbits of the UK-DMC1 satellite, using this underactuated controller, is shown in figure (13). The attitude is clearly stabilized in nadir pointing mode on all three axes. There is a small periodic deviation of the attitude, which is of ± 4 to 5 degrees on the actuated axes and ± 1.5 degree on the unactuated roll axis. When the underactuated controller is activated, attitude errors of 1.8 degree on the roll axis and 10 degrees on the yaw axis had to be performed and an accuracy of ± 0.5 degrees on all three axes was obtained after less than half an orbit. The periodic deviations from the required attitude (highlighted by rectangles in figure (13)) are only temporary and were found to coincide with the polar region of the satellite’s orbit, where magnetic disturbance torques can be significant. The fact that the controller regains nadir pointing after this disturbance suggests that the proposed singular controller robustly stabilizes the system. Figure (14) confirms that the magnetic torquing was turned off during the underactuated control mode.

The sun tracking performance in figure (10) was not as good as predicted in theory and although nadir pointing performance in figure (13) was relatively better, the difference between theoretical and experimental results is not fully explained by the aforementioned perturbation effects. Other factors such as model uncertainty and sensor noise should have been accounted for in the controller design. While numerical

simulations helped determine an initial set of controller parameters, these gains required further tuning to improve control performance. It was also found that enhancing settling time on the unactuated axis was a competing objective with the slew rate on the actuated axes. A better understanding of controller tuning may in the future be reached by theoretically analyzing control performance in the presence of uncertainties, noise and external disturbances with known bounds. The simplifying assumption of a zero total angular momentum, which implies that $\omega_3(0) = 0$, is also believed to be the source of bounded errors, as theoretically predicted in a paper by Horri and Hodgart.¹⁵ The momentum on the unactuated axes was indeed small but non zero during the experiments. Also, one of the safety conditions under which the experiments were authorized was to operate one of the two wheels in a small but nonzero momentum. This, together with controller tuning, which prioritized the unactuated axis control, partly explains the bounded but significant tracking errors during the sun tracking experiment. Another contribution to the small but nonzero momentum was the effect of the orbital rate, which was not included in the theoretical design. The attitude and angular velocities, which were applied in practice, were indeed expressed in the local orbit frame, because control objectives were specified in that frame.

The aim of these experiments was to demonstrate the possibility of achieving three axis stability using two reaction wheels. These experiments provide, as far as the authors know, the first practical demonstration of 3-axis attitude control by two control torques. It is however believed that the proposed underactuated controllers can also accommodate more challenging attitude maneuvers than those shown in this paper's experiments. In particular, the performance of the underactuated control approach based on the minimum norm optimization of the angular velocity tracking law is expected to enhance the results further. Indeed, numerical simulations have shown a 41 percent settling time enhancement in the fine pointing case, for similar integrated torque. This margin is significant enough to suggest that an enhancement should also be observed in orbit. Future work is therefore needed to provide a more complete analysis of the performance of the flight-tested controller, but also to practically demonstrate, at the next in-orbit testing opportunity, that the inverse optimal law based on angular velocity tracking can improve control performance.

VII. Conclusion

Two approaches have been successfully applied to the attitude of an underactuated satellite on all three axes : The first one was based on a perfect zero momentum assumption, while the other approach was based on angular velocity tracking. Three axis stability using the first approach has been successfully demonstrated in-orbit. Using a minimum norm inverse optimal technique, the angular velocity tracking approach was shown to potentially enhance attitude tracking performance in terms of settling time for a level of the integrated torque.

Acknowledgement

This work was supported by the European Union funded Marie Curie Astrodynamics research network. The authors would like to thank Dr Stephen Hodgart from the Surrey Space Centre for his useful advice and Dr Yoshi Hashida from Surrey Satellite Technology Limited for helping with the in-orbit testing of the control algorithms.

References

- ¹Brockett, R.W., "Asymptotic stability and feedback stabilization," *Differential Geometric Control Theory*, R.Smillman and H.H.Sussmann Editions, 1983, pp. 181-191.
- ²Crouch, P.E., "Spacecraft Attitude Control and Stabilization: Application of Geometric Control Theory to Rigid Body Models," *IEEE Transactions on Automatic Control*, Vol. 29, V0.4, 1984, pp. 321-331.
- ³Krishnan, H., McClamroch, H., Reyhanoglu, M., "On the Attitude Stabilization of a Rigid Spacecraft using Two Control Torques," American Control Conference, Chicago, IL, USA, 1992, pp. 1990-1995.
- ⁴Morin, P., "Robust Stabilization of the Angular Velocity of a Rigid Body with Two Controls," *European Journal of Control*, Vol. 1, 1996, pp. 51-56.
- ⁵Reyhanoglu, M., "Discontinuous Feedback Stabilization of the Angular Velocity of a Rigid Body with Two Control Torques," *Proceeding of the 35th Conference on Decision and Control*, Kobe, Japan, 1996.
- ⁶Aeyels, D., Szafranski, M., "Comments on the Stabilisability of the angular velocity of a rigid body," *Systems and Control Letters*, 1988, pp. 35-39.
- ⁷Astolfi, A., Rapaport, A., "Robust stabilization of the angular velocity of a rigid body," *Proceedings of the 36th IEEE Conference on Decision and Control*, 1997, pp. 2864-2869.
- ⁸Tsiotras, P., Longuski, J.M., "A new parameterization of the attitude kinematics", *The Journal of the Astronomical Sciences*, Vol.43, No.3, 1995, pp. 243-262.
- ⁹Tsiotras, P., Luo, J., "Control of underactuated spacecraft with bounded inputs," *Automatica*, Vol. 36, No. 8, 2000, pp. 1153-1169.
- ¹⁰Tsiotras, P., "Optimal regulation and passivity results for axisymmetric rigid bodies using two controls," *Journal of Guidance, Control and Dynamics*, Vol 20, No. 03, June 1997, pp.457-464.
- ¹¹Tsiotras, P., Doumtchenko, V., "Control of spacecraft subject to actuator failures : State of the art and open problems," *Journal of the Astronautical Sciences*, Vol. 48, No. 2-3, 2000, pp. 337-358.
- ¹²Hall, J.S.; Romano, M.; Cristi, R., "Quaternion Feedback Regulator for Large Angle Maneuvers of Underactuated Spacecraft," *American Control Conference*, Marriott Waterfront, Baltimore, MD, USA, 30 June- 02 July 2010.
- ¹³Godhavn, J-M., Egeland, O., "Attitude control of an underactuated satellite," *34th IEEE Conference on Decision and Control*, New Orleans, USA, 1996.
- ¹⁴Kim, S., Kim, Y., "Sliding Mode Tracking Control Law of Underactuated Axisymmetric Spacecraft," *AIAA Guidance, Navigation and Control Conference*, Denver, Colorado, USA, August 2000.
- ¹⁵Horri, N.M., Hodgart, M.S., "Attitude control of an underactuated small satellite," *IEEE Aerospace Conference*, Big Sky, Montana, USA, March 2003.

¹⁶Kim, S., Kim, Y., "Sliding mode stabilizing control law of underactuated spacecraft," *AIAA Guidance , Navigation and Control Conference and Exhibit*, Denver, CO, 14-17 August 2000.

¹⁷Yamada, K., Yoshikawa, S., Yamagushi, I., "Feedback attitude control of a spacecraft by two reaction wheels," *21st International Symposium on space Technology and Science* , Omiya , Japan , 1998.

¹⁸Terui, F., Motohashi, S., Fujiwara, T., Noda, A., Sako, N., Nakasuka, A., "Attitude manoeuvre of a bias momentum micro satellite using two wheels," *22nd International Symposium on Space Technology and Science* , Morioka , Japan , 2000.

¹⁹Seol, I-H., Leeghiml, H., Leel, D-H., Bang, H., "Momentum transfer control of a spacecraft with two Wheels by feedback linearization," *International Conference on Control, Automation and Systems*, Seoul, Korea, 14-17 October 2008.

²⁰Ake, T.B., Class, B.F., Roberts, B.A., Kruk, J.W., Blair, W.P., Moos, H.W., "Recovery of FUSE attitude control with two reaction wheels and magnetic torquer bars," *200th American Astronomical Society meeting*, Albuquerque, NM, June 2002.

²¹Freeman, F.A., Kokotovic, P.V., "Inverse Optimality in Robust Stabilization," *SIAM Journal on Control and Optimization*, vol. 34, no4, July 1996, pp. 1365-1391.

²²Bharadwaj, S., Qsipchuk, M., Mease, K.D., Park, F.C., "Geometry and Inverse Optimality in Global Attitude Stabilization," *AIAA Journal of Guidance, Control and Dynamics*, vol. 21, no. 6, 1998, pp. 930-939.

²³Krstic, M., Tsiotras, P., "Inverse Optimal Stabilization for a Rigid Spacecraft," *IEEE Transactions on Automatic Control*, Vol. 44, No. 5, 1999, pp. 1042-1049.

²⁴Horri, N.M., Palmer, P.L., Roberts,M., "Practical Implementation of Inverse Optimal Satellite Attitude Control," *21st International Symposium on Space Flight Dynamics (ISSFD)*, Toulouse, France, 28 Sep.- 2 oct., 2009.

²⁵Freeman, F.A., Kokotovic,P.V., "Inverse Optimality in Robust Stabilization," *SIAM Journal on Control and Optimization*, Vol. 34, No4, July 1996, pp. 1365-1391.

²⁶Wie, B., Weiss, H., "Quaternion Feedback for Spacecraft Large Angle Maneuvers," *AIAA Journal of Guidance, Control and Dynamics* , Vol 8, No3, 1985, pp.360-365.

²⁷Horri, N.M., Palmer, P., Roberts, M., "Optimal Satellite Attitude Control: A Geometric Approach," *Proceedings of the 2009 IEEE Aerospace Conference*, Big Sky, Montana, March 2009.

²⁸Horri, N.M., Palmer, P.L., Roberts, M., "Design and Validation of Geometric Optimisation Software for the Attitude Control of Microsatellites," *61st International Astronautical Congress*, IAC-10.C1.4.2, Prague, Czech republic, 27 Sep.- 1 Oct., 2010.

²⁹Khalil, H.K., "Lyapunov Stability," *Nonlinear Systems*, 3rd ed., Prentice Hall, Englewood Cliffs, NJ, 2002, pp.126-132.